

# Finite element solution of stress and flexural strength of functionally graded doubly curved sandwich shell panel

Sushmita Dash<sup>1a</sup>, Kulmani Mehar<sup>2b</sup>, Nitin Sharma<sup>3c</sup>, Trupti Ranjan Mahapatra<sup>4d</sup>  
and Subrata Kumar Panda<sup>\*5</sup>

<sup>1</sup>Department of Mechanical Engineering, GITA, Bhubaneswar, 752054, Odisha, India

<sup>2</sup>Mechanical Engineering Department, MITS, Madanapalle, Andhra Pradesh, India

<sup>3</sup>School of Mechanical Engineering, KIIT, Bhubaneswar, 751024, Odisha, India

<sup>4</sup>Department of Production Engineering, Veer Surendra Sai University of Technology (VSSUT), Burla, 768018, Odisha, India

<sup>5</sup>Department of Mechanical Engineering, NIT, Rourkela, 769008, Odisha, India

(Received October 31, 2018, Revised November 28, 2018, Accepted December 2, 2018)

**Abstract.** The finite solutions of deflection and the corresponding in-plane stress values of the graded sandwich shallow shell structure are computed in this research article via a higher-order polynomial shear deformation kinematics. The shell structural equilibrium equation is derived using the variational principle in association with a nine noded isoparametric element (nine degrees of freedom per node). The deflection values are computed via an own customized MATLAB code including the current formulation. The stability of the current finite element solutions including their accuracies have been demonstrated by solving different kind of numerical examples. Additionally, a few numerical experimentations have been conducted to show the influence of different design input parameters (geometrical and material) on the flexural strength of the graded sandwich shell panel including the geometrical configurations.

**Keywords:** functionally graded sandwich panels; HOSDT; variational principle; FEM

## 1. Introduction

In order to improve of expedient structural characteristics, the properties of individual constituents of engineering materials i.e., the metals and the ceramics are used in combination to achieve a heterogeneous composite material termed as functionally graded materials (FGMs). The FGMs have an inherent advantage over the conventional laminated and sandwich composite structures in the sense that the variation in the properties is continuous and smooth in the preferred directions. The directional control over the properties is attained by varying the volume fractions of two or more materials spatially. As a result of this, the FGM structure/structural components are devoid of delamination which is often observed in layered composite structures due to material discontinuities at the lamina interfaces. Thus, the failure of the load transfer mechanism owing to the concentration of inter-laminar

stresses leading to reduced stiffness. This, in leads, to the lower overall structural strength and the functional failure of the structures is circumvented. Therefore, graded or the graded sandwich structural components are favorably found in numerous high-performance engineering applications specifically as thermal-barrier systems. Recently the FG/FG-sandwich structures have also achieved considerable attention as vital elements for future power generation and high speed spacecraft industries (Vinson 2001). Several experimental, analytical and numerical studies have been conducted to recognize the static and dynamic characteristics of FG sandwich panels using various existing and modified kinematic models in the past (Jha *et al.* 2012, Bousahla *et al.* 2016, Boukhari *et al.* 2016, Boudierba *et al.* 2016, El-Haina *et al.* 2017, Bellifa *et al.* 2016). An extensive review of the diverse existing and improved theories (classical (CPT) (Ghannadpour *et al.* 2012, Ovesy *et al.* 2015), first-order (FOSDT) and higher order shear deformation theory (HOSDT) (Sherafat *et al.* 2013, Baseri *et al.* 2016, Bousahla *et al.* 2014, Ait Yahia *et al.* 2015, Sekkal *et al.* 2017, Menasria *et al.* 2017, Karami *et al.* 2018, Zine *et al.* 2018), hybrid theories and 3D elasticity techniques are employed for the modeling and analysis of the FG plates and shells have been presented by Thai and Kim (2015). A simpler modified FOSDT with fewer unknowns for analyzing the flexural behavior of FG sandwich plates has also been provided by Thai *et al.* (2014), Abdelaziz *et al.* (2011) obtained the closed form solution for the static responses of FG sandwich plates using a four-unknown based HOSDT together with Navier method. Lok and Cheng (2001) also presented the closed

\*Corresponding author, Associate Professor  
E-mail: call2subrat@gmail.com, pandask@nitrrkl.ac.in

<sup>a</sup>Research Scholar  
E-mail: gungunsushmita@gmail.com

<sup>b</sup>Assistant Professor  
E-mail: kulmanimehar@gmail.com

<sup>c</sup>Assistant Professor  
E-mail: nits.iiit@gmail.com

<sup>d</sup>Associate Professor  
E-mail: trmahapatra\_pe@vssut.ac.in

form solution for the forced response of truss-core thick sandwich panels by using the Rayleigh-Ritz method. Mezziane *et al.* (2014) analysed the buckling and free vibration responses of FG sandwich flat panels by considering the nonlinear variations in the in-plane displacement over the thickness of the panels. The inevitability of the HOSDT for predicting bending responses of laminated composite and sandwich flat panels analytically have been revealed by Kant and Swaminathan (2012). Analytical 3-D elasticity solution for the sandwich panels with FG core subjected to transverse loading has also been derived (Anderson 2003). Zenkour (2005a) implemented a sinusoidal shear deformation plate theory for computing the bending responses of FG sandwich flat panels with ceramic core. Later, this approach has been further extended to study the buckling and free vibration of FG sandwich plates (Zenkour 2005b). Additionally, a refined trigonometric HOSDT has also been presented for the flexural analysis of simply supported ceramic-metal FG sandwich plates (Zenkour 2013). Kashtalyan and Menshykova (2007) performed 3D elasticity analysis of sandwich panels with FG core subjected to transverse loading. We also note the use of finite element method (FEM) for the bending and vibration analysis of FG sandwich panel structures. Natarajan and Ganapathi (2012) analysed the bending and free vibration behaviour of FG sandwich plates based on a HOSDT with 13 degrees of freedom and employed an eight-noded quadrilateral element for discretization purpose Das and Barut (2006) studied the thermo-mechanical behaviour of thick sandwich panels with FG core by using a triangular third order shear deformation theory (TOSDT). Yang *et al.* (2008) utilized a perturbation technique in conjunction with Galerkin method to study the nonlinear bending responses of FG sandwich panels in the frame work of FOSDT. A comparative study on the thermomechanical bending of FG sandwich structures using the CPT, the FOSDT and TOSDT has also been reported (Zenkour and Alghamdi 2010). Also, the size dependent bending (Kolahchi and Heydari 2015), nonlinear bending, vibration and post-buckling analysis of sandwich which plates with FG sheets resting on elastic foundation have also been performed (Wang and Shen 2011). Further, various types of refined theories (Bennoun *et al.* 2016, Draiche *et al.* 2016, Bellifa *et al.* 2017, Attia *et al.* 2018, Fourn *et al.* 2018), higher-order shear and normal deformation theories (Houari *et al.* 2013, Mahi *et al.* 2015, Belabed *et al.* 2014, Mahmoudi *et al.* 2018, Belabed *et al.* 2018, Ayache *et al.* 2018, Benadouda *et al.* 2018) and unified shear deformation plate theory (Zenkour and Alghamdi 2008) have also been utilized every now and then to study the elastic/thermoelastic bending of FG sandwich panels. Researchers have also utilized higher-order zigzag theories (Kolahchi *et al.* 2017a) to study the bending responses of FG sandwich flat rectangular (Neves *et al.* 2012) and circular (Alipour and Shariyat 2012) plate structures. Several studies considering the stretching effect (Chaht *et al.* 2015, Hamidi *et al.* 2015, Abualnour *et al.* 2018, Younsi *et al.* 2018) with an aim of accurately estimating the flexural behaviour of the structure have also been reported. Neves *et al.* (2012) utilized a mesh-less

technique in the framework of quasi-3D HOSDT to analyse the static, free vibration and buckling responses of sandwich FG plates. Nguyen-Xuan *et al.* (2013) utilised a fifth-order shear deformation theory in conjunction with isogeometric FE to investigate the vibration and bending responses of laminated composite sandwich plates. Sobhy and Zenkour (2015) studied the influence of time harmonic sinusoidal variation of temperature over the surface and variation through thickness on the bending characteristics of FG sandwich plates resting on Pasternak's foundation. Also, the studies on flexural and free vibration responses of composite sandwich panels reinforced with CNT have been reported in the past (Natarajan *et al.* 2014). Kolahchi and his colleagues (Kolahchi 2017, Kolahchi and Arani 2016, Kolahchi *et al.* 2017b, Kolahchi *et al.* 2016) studied the buckling, bending and vibration behaviour of laminated nanoplates using several refined theories.

The brief review of literature reveals that the FG sandwich panels have been extensively studied for their flexural and free-vibration responses by using various analytical/numerical/mesh-free techniques in the framework of several mid-plane kinematic theories. However, majority of the studies consider flat panels only and the doubly curved (cylindrical, spherical, elliptical and hyperboloid) FG sandwich shell panel structures have got less attention. Based on the author's knowledge, numerical studies pertaining to the flexural characteristics of FG sandwich curved panels implementing HOSDT via FEM are yet to be reported. In the current study, the flexural characteristics of curved FG shell panel structures are investigated in the framework of the HOSDT with nine-degrees of freedom in conjunction with FEM. A nine-noded quadrilateral isoparametric element is utilized for discretization purpose. After testing the stability and efficacy of the proposed scheme through convergence and validation studies, numerous numerical results are provided to investigate the influence of various geometrical factors and material parameters on the flexural characteristics of FG sandwich curved panel structures. The useful inferences are brought out by solving appropriate numerical examples.

## 2. Formulation and solution technique

A general mathematical formulation for obtaining the flexural responses of doubly curved functionally graded sandwich shell panels is derived. The core is considered to be purely ceramic whereas the face sheets have material graded (from ceramic to metal) functionally along the thickness direction. The material properties (young's modulus, density and Poisson's ratio) vary as per the following relation

$$P(z) = P_m + (P_c - P_m)V_f^{(n)} \quad (1)$$

where,  $P_m$  and  $P_c$  are the material properties of metal and ceramic, respectively,  $V_f^{(n)}$  is the volume fraction of the ceramic ( $n=1,2,3$ ). The volume fraction of the ceramic varies through the thickness as per the following power-law

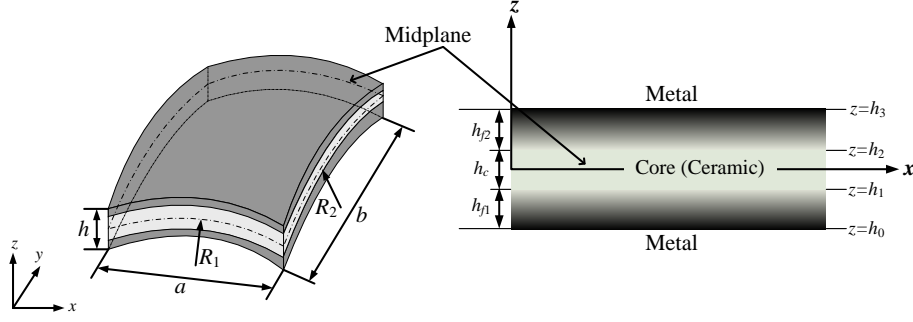


Fig. 1 Geometry and material variation in FG sandwich curved panels with ceramic core

$$\left. \begin{aligned} V_f^{(1)} &= \left( \frac{z-h_0}{h_1-h_0} \right)^k, z \in [h_0, h_1] \\ V_f^{(2)} &= 1, z \in [h_1, h_2] \\ V_f^{(3)} &= \left( \frac{z-h_3}{h_2-h_3} \right)^k, z \in [h_2, h_3] \end{aligned} \right\} \quad (2)$$

where, the thickness coordinate ( $z$ ) levels  $h_0$ ,  $h_1$ ,  $h_2$  and  $h_3$  are defined in Fig. 1 which illustrates the geometry of the shell panels based on the principal radii of curvature along the longitudinal and transverse directions.

In the present analysis, curved panels with dimensions ( $a \times b \times h$ ) m<sup>3</sup> and having a rectangular base (projection of the curved panel would be a rectangle) are considered. The thickness of the core is denoted as “ $h_c$ ” whereas the thickness of the bottom and top face sheets are denoted as “ $h_{f1}$ ” and “ $h_{f2}$ ”, respectively such that  $h = h_c + h_{f1} + h_{f2}$ . The principal radius of curvature along  $x$  and  $y$  direction is  $R_1$  and  $R_2$ , respectively. The curved panel geometries are defined as: cylindrical ( $R_1=R$ ,  $R_2=\infty$ ), spherical ( $R_1=R$ ,  $R_2=R$ ), elliptical ( $R_1=R$ ,  $R_2=2R$ ), hyperboloid ( $R_1=R$ ,  $R_2=-R$ ) and flat ( $R_1=R_2=\infty$ ) on the basis of curvature, where  $R$  is a constant. The displacement field ( $p$ ,  $q$  and  $r$ ) of the FG shell panel i.e., the displacements of a point along the  $x$ ,  $y$  and  $z$  coordinates based on the HOSDT kinematic relation is expressed as (Kant and Swaminathan 2002)

$$\left. \begin{aligned} p(x, y, z) &= p_0(x, y) + zp_1(x, y) + z^2 p_2(x, y) + z^3 p_3(x, y) \\ q(x, y, z) &= q_0(x, y) + zq_1(x, y) + z^2 q_2(x, y) + z^3 q_3(x, y) \\ r(x, y, z) &= r_0(x, y) \end{aligned} \right\} \quad (3)$$

where,  $p_0$ ,  $q_0$  and  $r_0$  are the mid-plane displacements of a point with respect to corresponding coordinates.  $p_1$  and  $q_1$  are the rotations of transverse normal about the  $y$ - and  $x$ -axes, respectively. The higher-order functions  $p_2$ ,  $q_2$ ,  $p_3$  and  $q_3$  defined in the mid-plane of the shell are involved in present displacement field.

Now, the strain displacement field can be expressed as

$$\left\{ \varepsilon \right\} = \left\{ \varepsilon_{xx} \quad \varepsilon_{yy} \quad \gamma_{xy} \quad \gamma_{xz} \quad \gamma_{yz} \right\} = \left\{ \begin{aligned} &\left( \frac{\partial p}{\partial x} + \frac{r}{R_1} \right) \quad \left( \frac{\partial q}{\partial y} + \frac{r}{R_2} \right) \quad \left( \frac{\partial p}{\partial y} + \frac{\partial q}{\partial x} + \frac{2r}{R_{12}} \right) \dots \\ &\dots \left( \frac{\partial p}{\partial z} + \frac{\partial r}{\partial x} - \frac{p}{R_1} \right) \quad \left( \frac{\partial q}{\partial z} + \frac{\partial r}{\partial y} - \frac{q}{R_2} \right) \end{aligned} \right\} \quad (4)$$

By substituting Eq. (3) in Eq. (4), the strain vector can further be given as

$$\left\{ \varepsilon \right\} = \left\{ \begin{matrix} \varepsilon_{xx} \\ \varepsilon_{yy} \\ \gamma_{xy} \\ \gamma_{xz} \\ \gamma_{yz} \end{matrix} \right\} = \left\{ \begin{matrix} \varepsilon_x^0 \\ \varepsilon_y^0 \\ \varepsilon_{xy}^0 \\ \varepsilon_{xz}^0 \\ \varepsilon_{yz}^0 \end{matrix} \right\} + z \left\{ \begin{matrix} k_x^1 \\ k_y^1 \\ k_{xy}^1 \\ k_{xz}^1 \\ k_{yz}^1 \end{matrix} \right\} + z^2 \left\{ \begin{matrix} k_x^2 \\ k_y^2 \\ k_{xy}^2 \\ k_{xz}^2 \\ k_{yz}^2 \end{matrix} \right\} + z^3 \left\{ \begin{matrix} k_x^3 \\ k_y^3 \\ k_{xy}^3 \\ k_{xz}^3 \\ k_{yz}^3 \end{matrix} \right\} \quad (5)$$

The Eq. (5) can further be expressed as

$$\left\{ \varepsilon \right\} = [T] \left\{ \hat{\varepsilon} \right\} \quad (6)$$

where,  $\left\{ \hat{\varepsilon} \right\} = \left\{ \varepsilon_x^0 \quad \varepsilon_y^0 \quad \varepsilon_{xy}^0 \quad \varepsilon_{xz}^0 \quad \varepsilon_{yz}^0 \quad k_x^1 \quad k_y^1 \quad k_{xy}^1 \quad k_{xz}^1 \quad k_{yz}^1 \quad k_x^2 \quad k_y^2 \quad k_{xy}^2 \quad k_{xz}^2 \quad k_{yz}^2 \quad k_x^3 \quad k_y^3 \quad k_{xy}^3 \quad k_{xz}^3 \quad k_{yz}^3 \right\}^T$

is the mid-plane strain vector and  $[T]$  is the function of thickness coordinate.

The present shell panel model is discretised using a nine noded quadrilateral Lagrangian isoparametric element with nine degrees of freedom associated with each node.

The elemental displacement vector is expressed as

$$\left\{ \lambda_0 \right\} = \sum_{i=1}^9 N_i \left\{ \lambda_{0i} \right\} \quad (7)$$

where,  $\left\{ \lambda_{0i} \right\} = \left\{ p_{0i} \quad q_{0i} \quad r_{0i} \quad p_{1i} \quad q_{1i} \quad p_{2i} \quad q_{2i} \quad p_{3i} \quad q_{3i} \right\}^T$  is the nodal displacement vector at node  $i$ .  $N_i$  is the shape function for the  $i^{th}$  node and the details can be seen in (Cook *et al.* 2000).

The mid-plane strain vector as expressed in Eq. (6) can be rewritten in terms of nodal displacement vectors as

$$\left\{ \hat{\varepsilon} \right\} = [B] \left\{ \lambda_{0i} \right\} \quad (8)$$

where,  $[B]$  is the product form of differential operators and the shape functions in the strain terms. Thus, the stress-strain relationship for the FG shell panel can be expressed as

$$\left\{ \sigma \right\} = [\bar{Q}] \left\{ \varepsilon \right\} \quad (9)$$

where,  $\left\{ \sigma \right\} = \left\{ \sigma_{xx} \quad \sigma_{yy} \quad \tau_{xy} \quad \tau_{xz} \quad \tau_{yz} \right\}^T$  is stress vector and  $[\bar{Q}]$  is the reduced stiffness matrix.

The strain energy of the curved shell panel can be expressed as

$$U = \frac{1}{2} \int_V \{\varepsilon\}^T \{\sigma\} dV \quad (10)$$

Eq. (10) can be rewritten by substituting strains and stresses from Eqs. (6) and (9) and conceded as

$$U = \frac{1}{2} \int_A \left( \{\bar{\varepsilon}\}^T [D] \{\bar{\varepsilon}\} \right) dA \quad (11)$$

where,  $[D] = \int_{-h/2}^{+h/2} [T]^T [\bar{Q}] [T] dz$ .

The elemental form of strain energy (as given by Eq. (11)) can be rearranged by substituting Eq. (8) in it to have the following form

$$U_e = \frac{1}{2} \int_A \left( \{\lambda_{0_i}\}^T [B]^T [D] [B] \{\lambda_{0_i}\} \right) dA \quad (12)$$

Eq. (12) can further be expressed as

$$U_e = \frac{1}{2} \{\lambda_{0_i}\}^T [K_e] \{\lambda_{0_i}\} \quad (13)$$

where,  $[K_e] = \int_{-1}^1 \int_{-1}^1 [B]^T [D] [B] |J| d\xi d\eta$  is the elemental stiffness matrix.

The total work done by externally applied load ( $q$ ) can be expressed as

$$P = \iint \{\lambda_{0_i}\}^T \{\bar{q}\} dx dy \quad (14)$$

The elemental form of work done by the applied load is given as

$$P_e = \{\lambda_{0_i}\}^T \{F_e\} \quad (15)$$

where,  $\{\lambda\}$  is the global displacement vector and  $\{F_e\}$  is the elemental force vector as a result of the mechanical load.

The final form of governing equation of the FG shell panel is derived using variational principle which is designated as

$$\delta \Pi_e = \delta U_e - \delta P_e = 0 \quad (16)$$

where,  $\delta$  is the variational symbol and  $\Pi_e$  is the elemental potential energy.

The global form of the equilibrium equation for static analysis is obtained by substituting Eqs. (13) and (15) in Eq. (16) and conceded as

$$[K] \{\lambda\} = \{F\} \quad (17)$$

where,  $[K]$  is the global stiffness matrix and  $\{F\}$  is the global mechanical load vector. Eq. (17) is solved to obtain the deflection of the system.

### 3. Result and discussion

The flexural responses of curved higher-order FG sandwich shell panels are computed through a domestic FE code developed in MATLAB environment. The cylindrical,

Table 1 Material properties used in the analysis

	Aluminium	Alumina	Zirconia
Young's modulus ( $E$ , GPa)	70	380	151
Poisson's ratio ( $\nu$ )	0.3	0.3	0.3

Table 2 Configuration in different FG sandwich panel symmetries

Symmetry	$h_0$	$h_1$	$h_2$	$h_3$
1-2-2	$-h/2$	$-3h/10$	$h/10$	$h/2$
1-1-3	$-h/2$	$-3h/10$	$-h/10$	$h/2$
2-1-4	$-h/2$	$-3h/14$	$-h/14$	$h/2$
2-1-3	$-h/2$	$-h/6$	0	$h/2$
4-1-3	$-h/2$	0	$h/8$	$h/2$

spherical, elliptical, hyperboloid and flat shell panel geometries are considered for the current study. The static analysis is conducted for two combinations of metal and ceramic materials namely, Aluminium/Alumina [Al/Al<sub>2</sub>O<sub>3</sub>] and Aluminium/Zirconia [Al/ZrO<sub>2</sub>]. The material properties of the metal and the ceramic in the aforementioned combinations are mentioned in Table 1 (Lok and Cheng 2001).

The FG sandwich panels are subjected to the sinusoidal load applied on the surface and given as

$$\bar{q}(x, y) = \bar{q}_0 \sin(\pi x/a) \sin(\pi y/b) \quad (18)$$

where,  $\bar{q}_0$  is the load intensity at the panel center.

The symmetry of FG panels is defined in terms of the ratio of face and core thickness and represented as  $h_{f1}-h_c-h_{f2}$ . The various symmetry schemes of the panels considered in the present analysis are summarized in Table 2. The variation of volume fraction along the panel thickness for various power-law indexes are also portrayed in Fig. 2.

The solutions are computed using different sets of support conditions in the combination of clamped (C), simply-supported (S) and free (F) supports to avoid rigid body motion and to reduce the number of unknowns. The restricted field of variables at the panel edges corresponding to each condition are given as:

- Simply-supported (S)  $x=0, a$   $q_0=r_0=q_1=q_2=q_3=0$   
 $y=0, b$   $q_0=r_0=p_1=p_2=p_3=0$
- Clamped (C)  $x=0, a$   $p_0=q_0=r_0=p_1=q_1=$   
 $y=0, b$   $p_2=q_2=p_3=q_3=0$
- Free (F)  $x=0, a$   $p_0=q_0=r_0=p_1=q_1=$   
 $y=0, b$   $p_2=p_2=p_3=q_3 \neq 0$

Based on this definition, the combinations end supports are utilized for the current numerical analysis i.e. (a) All sides simply supported [SSSS], (b) All sides clamped [CCCC], (c) Two opposite sides are simply supported and others free [SFSF], (d) Two opposite sides are simply supported and others clamped [SCSC], (e) Two opposite sides are clamped and others free [CFCF] and (f) Cantilever (one side clamped, others free) [CFFF]

The panels are assumed to have the following dimensions throughout, unless specified otherwise:  $h=0.005$  m,  $a/h=50$ ,  $a/b=1$ ,  $R/a=5$ . The core-face thickness ratio is defined as  $h_c/h_f$  wherein  $h=h_c+2h_f$ . The Aluminium-Alumina

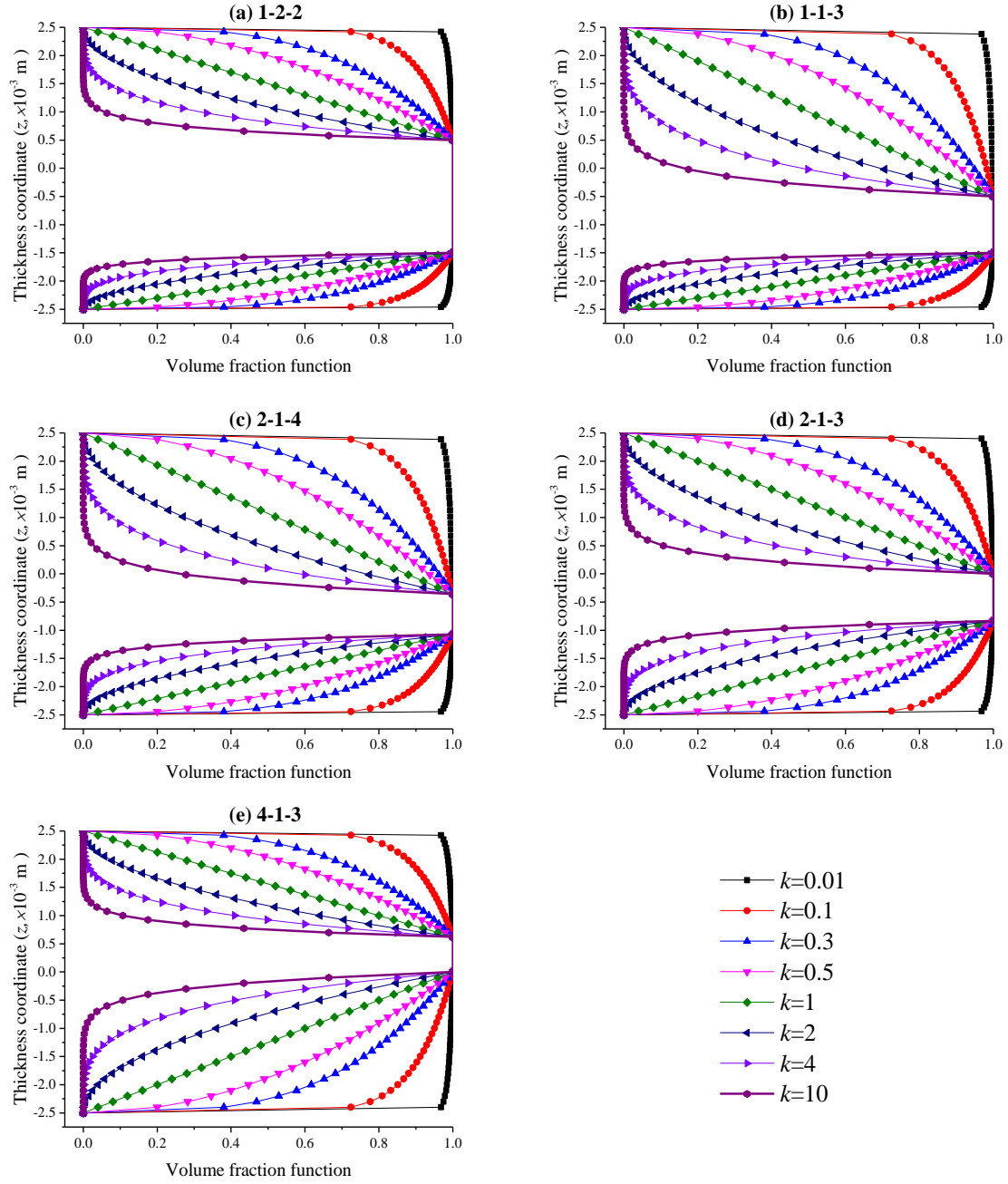


Fig. 2 Variation of volume fraction along the panel thickness for various power-law indexes: (a) 1-2-2, (b) 1-1-2, (c) 2-1-4, (d) 2-1-3, (e) 4-1-3 FG sandwich panel

(Al/Al<sub>2</sub>O<sub>3</sub>) material properties are utilized, if not stated explicitly. The central deflection is nondimensionalized as  $W=10hE_0r_{(a/2,b/2)}/a^2\bar{q}_0$ , where  $E_0=1$  GPa. The normal stress ( $\sigma_{xx}$ ) and transverse shear stress ( $\sigma_{xz}$ ) are nondimensionalized as  $\sigma'_{xx}=\frac{10h^2}{a^2\bar{q}_0}\sigma_{xx}(a/2,b/2,z)$  and

$\sigma'_{xz}=\frac{h}{a\bar{q}_0}\sigma_{xz}(0,b/2,z)$ , respectively. The convergence

behaviour of the model is tested and the validity of the results is first established. Subsequently, the model is extended to solve several numerical examples to investigate the influence of varying power-law index, thickness ratio,

aspect ratio, sandwich symmetry type, geometry, curvature ratio and support conditions on the flexural behaviour of FG sandwich curved panel structures under the influence of sinusoidal load.

### 3.1 Convergence study

Firstly, the stability of the presently developed model is tested through convergence study. The nondimensional central deflection values of simply-supported Aluminium-Alumina (Al/Al<sub>2</sub>O<sub>3</sub>) FG square sandwich shell panels of different geometries and subjected to sinusoidal distributed load are computed. Panels with geometrical specifications

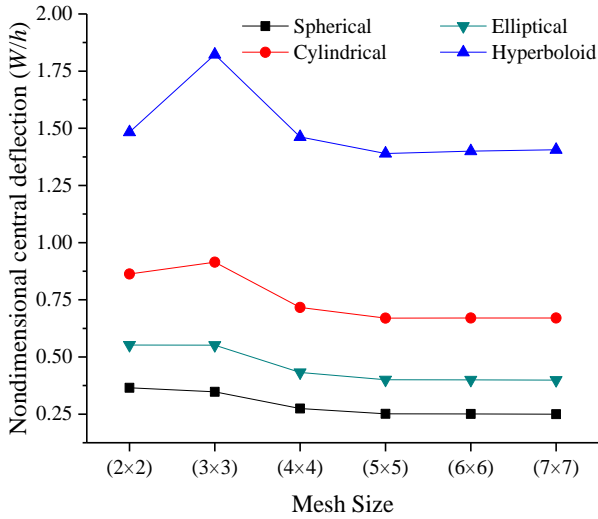


Fig. 3(a) Convergence behaviour for simply supported curved FG shell panels

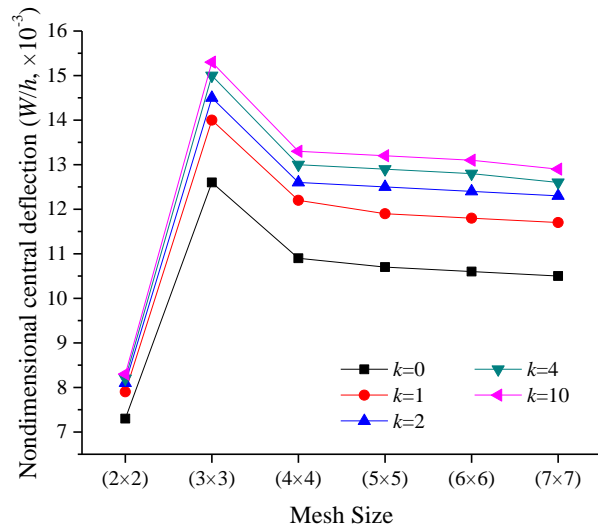


Fig. 3(b) Convergence behaviour for clamped cylindrical FG shell panels

as:  $h=0.005$  m,  $a/h=50$ ,  $R/a=5$ ,  $h_c/h_f=3$  and the load parameter=1MPa are considered. Fig. 3(a) depicts the variation of nondimensional central deflection ( $W/h$ ) values for  $k=5$  with increasing mesh size for the considered curved panel geometries. Further, clamped square cylindrical FG sandwich shell panels ( $h=0.005$  m,  $a/h=10$ ,  $R/a=20$ ,  $h_c/h_f=10$ ) composed of Aluminium-Zirconia ( $Al/ZrO_2$ ) are considered. The flexural responses are computed for increasing mesh size corresponding to  $k=0, 1, 2, 4$  and 10 and shown in Fig. 3(b). From both the examples it can clearly be observed that the model is showing excellent convergence rate with the mesh refinement and on the basis of the convergence studies, a  $(6 \times 6)$  mesh has been utilized for the computation of responses for throughout the analysis.

### 3.2 Validation study

In order to demonstrate the effectiveness of the present

Table 3 Comparison of nondimensional central deflection of simply supported FG sandwich flat panels

$k$	Theory	1-0-1	2-1-2	1-1-1	1-2-1	2-2-1
0	CPT (Zenkour 2005a)	0.1856	0.1856	0.1856	0.1856	0.1856
	TOSDT (Zenkour 2005a)	0.19606	0.19606	0.19606	0.19606	0.19606
	FOSDT (Zenkour 2005a)	0.19607	0.19607	0.19607	0.19607	0.19607
	Present (HOSDT)	0.1959	0.1959	0.1959	0.1959	0.1959
1	CPT (Zenkour 2005a)	0.3105	0.2942	0.2803	0.2596	0.2692
	TOSDT (Zenkour 2005a)	0.3236	0.3063	0.2920	0.2709	0.28085
	FOSDT (Zenkour 2005a)	0.3248	0.3075	0.2930	0.2717	0.28168
	Present (HOSDT)	0.3232	0.3059	0.2916	0.2706	0.2805
2	CPT (Zenkour 2005a)	0.3589	0.3394	0.3207	0.2910	0.30405
	TOSDT (Zenkour 2005a)	0.3734	0.3523	0.3329	0.3026	0.31617
	FOSDT (Zenkour 2005a)	0.3751	0.3541	0.3344	0.3037	0.31738
	Present (HOSDT)	0.3729	0.3519	0.3324	0.3022	0.3158
5	CPT (Zenkour 2005a)	0.40905	0.3916	0.37128	0.3495	0.33474
	TOSDT (Zenkour 2005a)	0.4112	0.39418	0.37356	0.35123	0.33631
	FOSDT (Zenkour 2005a)	0.39227	0.37789	0.35865	0.33693	0.32283
	Present (HOSDT)	0.4089	0.3915	0.3711	0.3343	0.3493
10	CPT (Zenkour 2005a)	0.3988	0.3894	0.3724	0.3361	0.34915
	TOSDT (Zenkour 2005a)	0.4177	0.4041	0.3855	0.3482	0.36215
	FOSDT (Zenkour 2005a)	0.4192	0.4066	0.3879	0.3500	0.36395
	Present (HOSDT)	0.4173	0.4038	0.3852	0.3478	0.3619

developed model for computing the flexural responses precisely, the central deflection obtained using the present scheme is compared with the benchmark results available in the open literature. The FG sandwich flat panel (simplest form of curved panels,  $R_1=R_2=\infty$ ) example as solved by Zenkour (2005a) is reproduced for the validation purpose. The central deflection values in nondimensional form are computed for 1-0-1, 2-1-2, 1-1-1, 1-2-1 and 2-2-1 symmetries flat panels ( $h=0.1$  m,  $a/b=1$ ,  $a/h=10$ ) corresponding to  $k=0, 1, 2, 5$  and 10. The comparison of present central deflection values with those reported by Zenkour (2005a) presented in Table 3 clearly shows the close conformance of the current results with the reference data. However, it is noted that the responses computed using the present model are lesser in comparison to the values reported by Zenkour (2005a). This is primarily attributed to the difference in theories utilized for modelling the panel structure. It is important to mark here that the present model is based on more general HOSDT kinematic relations and solved via FEM steps whereas the reference (Zenkour, 2005a) utilized CPT, TOSDT and FOSDT for structural modeling and computed the responses analytically.

Further, in order to build more confidence in the present model, the present nondimensional normal stress  $\sigma'_{xx}$  varying with the thickness coordinate  $z$  is compared with the values reported by Zenkour (2005a) obtained in the framework of TOSDT. Fig. 4(a) and (b) illustrate the



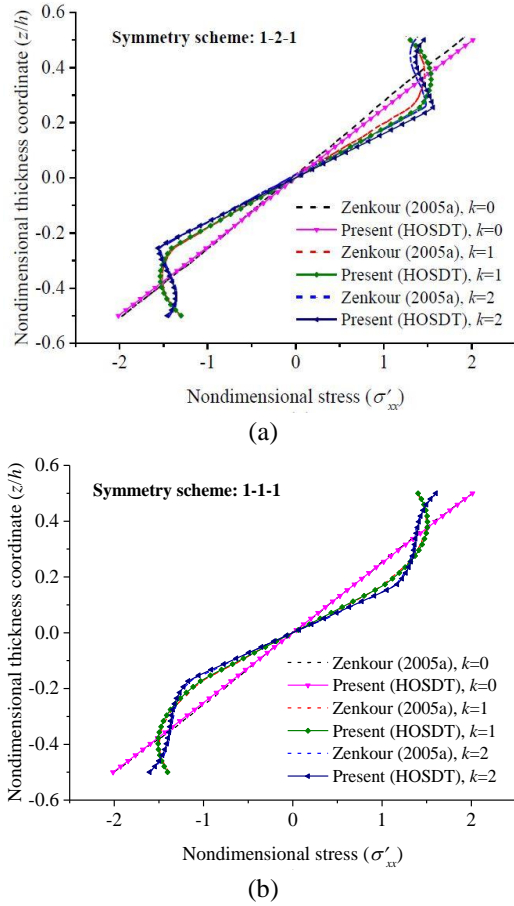


Fig. 4 Comparison of nondimensional normal stress varying with the thickness coordinate of the simply supported FG sandwich plate: (a) (1-2-1) scheme, (b) (1-1-1) scheme

variation of stress for 1-2-1 and 1-1-1 symmetries of the sandwich panels, respectively, corresponding to  $k=0, 1$  and  $2$ . It is evident that present values are in excellent agreement with the reference thereby justifying the correctness of the present results.

### 3.3 Numerical Illustrations

After having established the stability and validity of the proposed scheme, several numerical examples are now solved to understand the influence of different parameters such as power-law index ( $k$ ), geometry, aspect ratios ( $a/b$ ), curvature ratio ( $R/a$ ), thickness ratio ( $a/h$ ) and support conditions on the flexural responses of FG sandwich curved shell panels. The detailed discussion is mentioned in the following sub-sections.

#### 3.3.1 Effect of power law index

Simply supported FG sandwich curved shell panels of different geometries and diverse core-face thickness ratios ( $h_c/h_f=0, 0.5, 1, 2, 5, 10$ ) are analysed to observe the influence of varying power-law index ( $k=0, 0.5, 1, 2, 5, 10$ ) on the flexural responses. Fig. 5(a) and (b) indicate the central deflection values for spherical, elliptical and cylindrical, hyperboloid shell panels, respectively. It is observed that the deflection is same for a particular

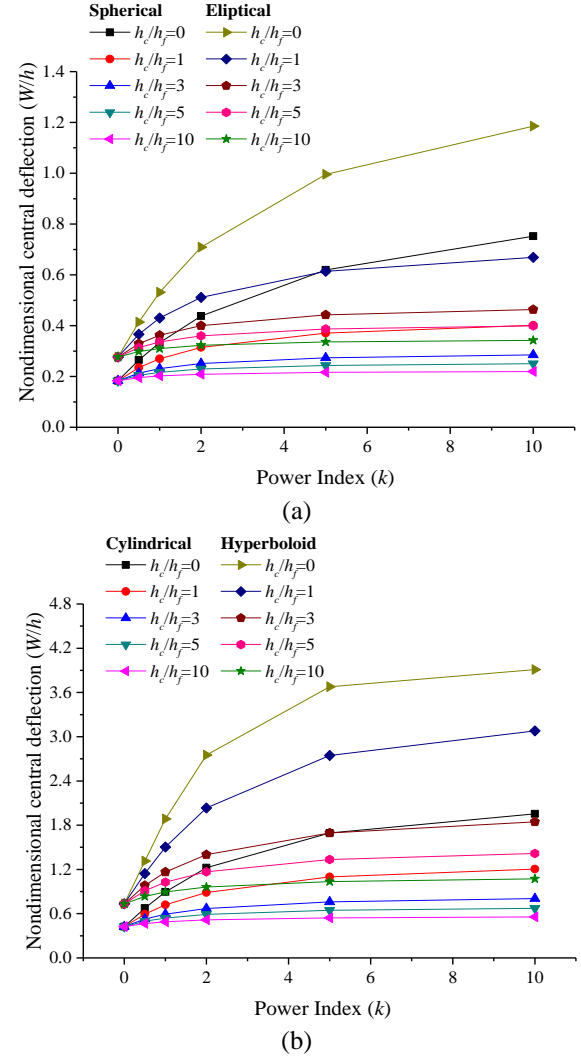


Fig. 5 Influence of power-law index on nondimensional central deflection: (a) Spherical and elliptical panels, (b) Cylindrical and hyperboloid panels

geometry corresponding to  $k=0$  irrespective of  $h_c/h_f$  values. However, the central deflection increases with increasing power-law index for all of the geometries considered and the increase in deflection is larger for panels with low core-face thickness ratio. Also, the increase in deflection with increasing power-law index dies out for higher  $h_c/h_f$  values as the panels become increasingly stiff owing to the ceramic core becoming thicker. This behaviour is observed in all the geometries considered. Moreover, the deflection is less in case of doubly curved panels (spherical and elliptical) compared to that in singly curved cylindrical panel and hyperboloid (having positive as well as negative curvature) panel and the same is evident from Figs. 6(a) and (b). As expected, the spherical panels have smaller deflection compared to elliptical panels as the presence of higher curvature along transverse direction makes the panels stiffer. Interestingly, cylindrical panels exhibit lesser deflection values as compared to hyperboloid panels.

Moreover, the variation of nondimensional normal stress ( $\sigma'_{xx}$ ) and transverse shear stress ( $\sigma'_{xz}$ ) along the thickness is obtained for  $k=0, 1, 5, 10$  and depicted in Fig. 6 for FG

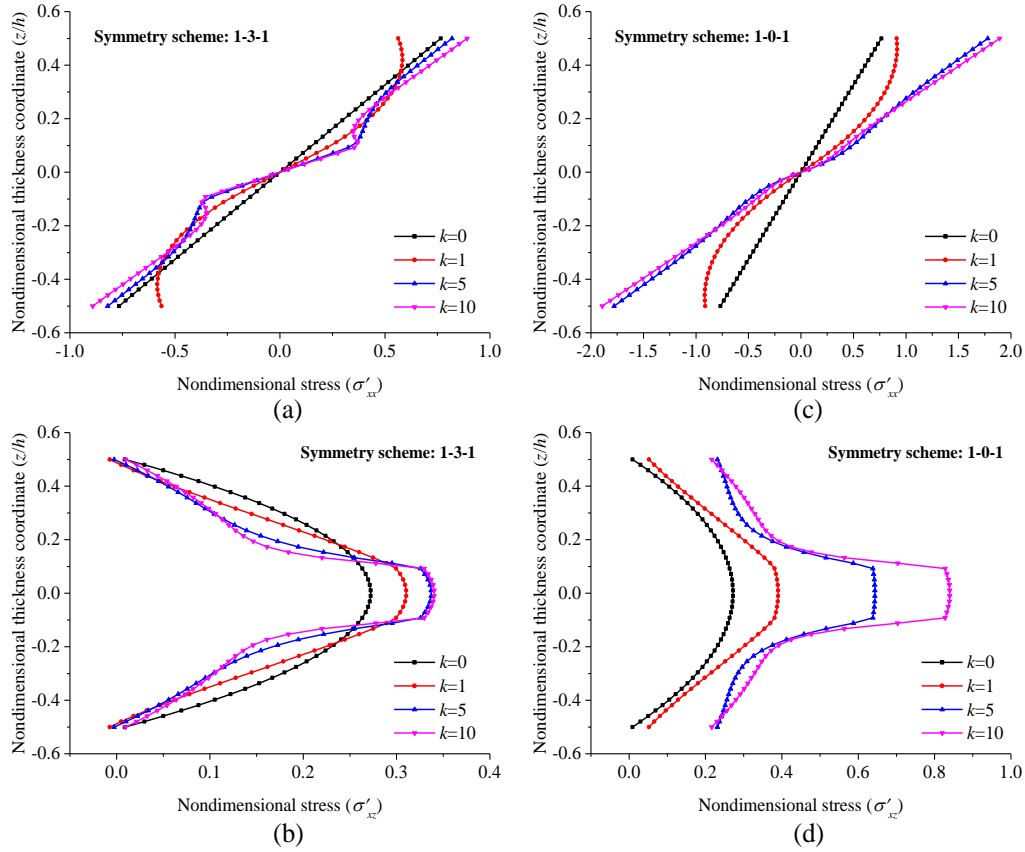


Fig. 6 Influence of power-law index on nondimensional stress: (a)  $\sigma'_{xx}$  for 1-3-1 scheme, (b)  $\sigma'_{xz}$  for 1-3-1 scheme, (c)  $\sigma'_{xx}$  for 1-0-1 scheme, (d)  $\sigma'_{xz}$  for 1-0-1 scheme

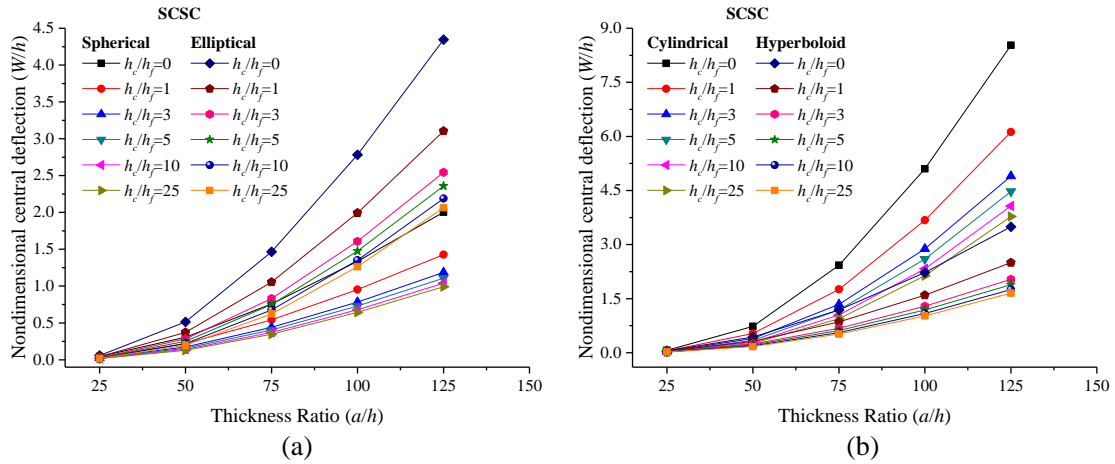


Fig. 7 Influence of thickness ratio index on nondimensional central deflection: (a) Spherical and elliptical panels, (b) Cylindrical and hyperboloid panels

sandwich flat panels having symmetry schemes 1-3-1 and 1-0-1. The normal stress is the more dominant compared to transverse shear stress.

### 3.3.2 Effect of thickness ratio

In this section the influence of thickness ratio ( $a/h$ ) on the flexural behaviour of FG sandwich ( $k=2$ ) curved panels under [SCSC] support condition is investigated. For computation purpose, the thickness ratio is varied (by keeping  $h$  constant) as  $a/h=25, 50, 75, 100$  and  $125$ . The

variation of central deflection with the  $a/h$  for the considered geometries corresponding to different core-face thickness ratios ( $h_c/h_f$ ) is illustrated in Fig. 7. It can be observed that the central deflection increases with increasing thickness ratio for all of the considered geometries. It is to be marked that the increase in central deflection with increasing thickness ratio is higher in the case of elliptical panels as compared to the spherical panels for a particular core-face thickness values. It is worthy to note that, the variation in central deflection is less



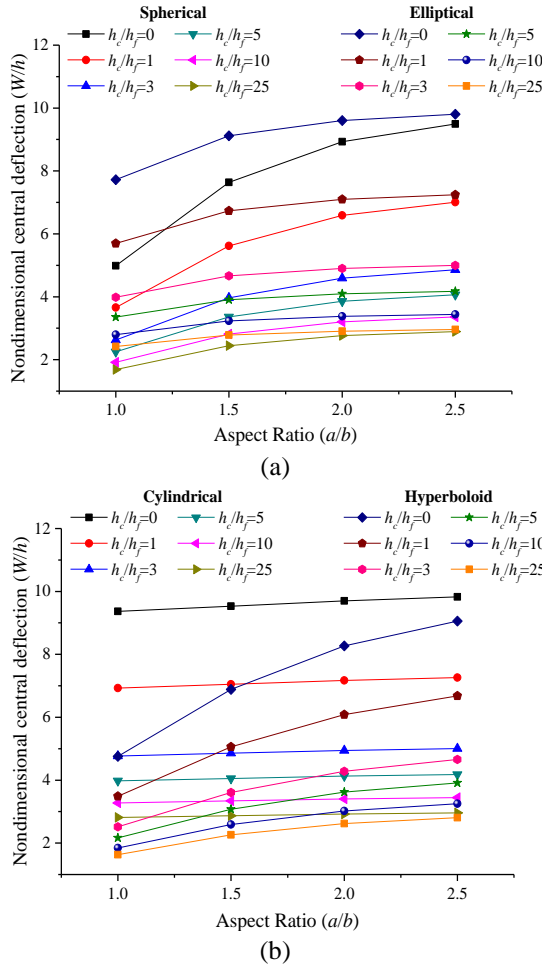


Fig. 8 Influence of aspect ratio on nondimensional central deflection: (a) Spherical and elliptical panels, (b) Cylindrical and hyperboloid panels

corresponding to lower thickness ratios and gradually increase for higher  $a/h$  values. A similar trend is observed in the case of cylindrical and hyperboloid panels and the same can be observed from Fig. 7(b). However, the maximum deflection (occurring for  $h_c/h_f=0$ ) for elliptical panels exceeds that for spherical panels by 53.87%. Similarly, in contrast with the trend observed in the example for varying power-law index, the deflection for hyperboloid panels exceeds the corresponding values for cylindrical panels. In the present case the maximum deflection for hyperboloid panel is 59.05% higher than that for the cylindrical panel.

### 3.3.3 Effect of aspect ratio

The influence of varying aspect ratio ( $a/b$ ) on the central deflection of curved sandwich panels is now investigated. For the present analysis, the dimension  $b$  is varied and  $a$  is kept constant such that  $a/b=1, 1.5, 2$  and  $2.5$ . The panels ( $k=2$ ) are considered to be under [CFCF] support condition and the responses are depicted in Fig. 8 (a) and (b). It is observed that the deflection of cylindrical panels is not influenced by varying aspect ratio. However, for other geometries, the deflection initially increases rapidly with increasing aspect ratio and exhibits asymptotic behaviour corresponding to higher aspect ratio values. Moreover, the

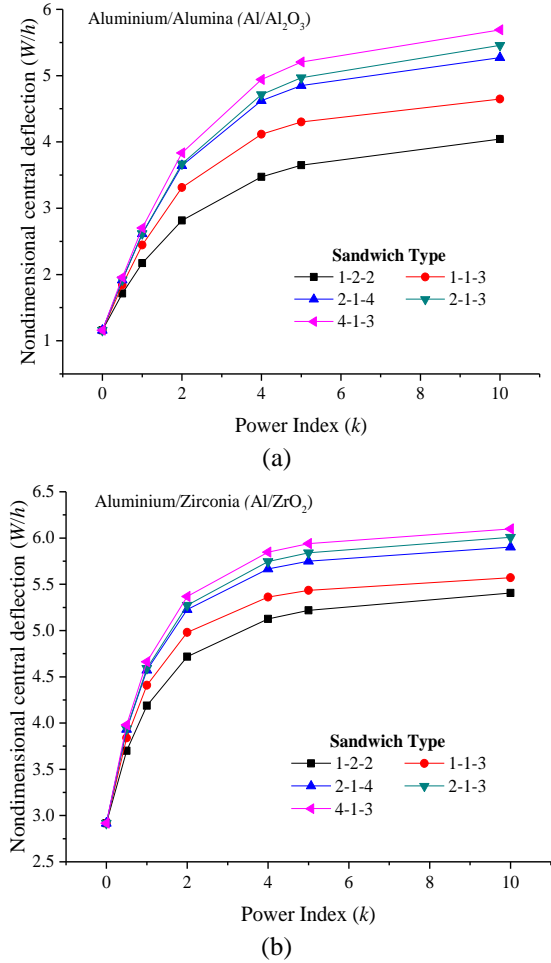


Fig. 9 Influence of sandwich symmetry type on nondimensional central deflection: (a) Aluminium/Alumina ( $Al/Al_2O_3$ ), (b) Aluminium/Zirconia ( $Al/ZrO_2$ )

variation in deflection is larger for panels with lower core-face thickness ratio.

### 3.3.4 Effect of sandwich symmetry type

It is expected that the stiffness of the sandwich panel will be significantly governed by the type of symmetry. Therefore, in this example simply supported square spherical sandwich shell panels ( $R/a=20$  and  $a/h=20$ ) with Aluminium/Alumina ( $Al/Al_2O_3$ ) and Aluminium/Zirconia ( $Al/ZrO_2$ ) material properties are considered for investigating the influence of sandwich symmetry type (1-2-2, 1-1-3, 2-1-4, 2-1-3 and 4-1-3) on the deflection behaviour. Fig. 9 (a) and (b) illustrates the variation of nondimensional central deflection for the considered schemes corresponding to  $Al/Al_2O_3$  and  $Al/ZrO_2$  material, respectively. It is evident that the deflection values are higher for  $Al/ZrO_2$  panels in comparison to the corresponding values for  $Al/Al_2O_3$ . This may be attributed to the lower stiffness of the Zirconia core. Further, for both of the materials, the 4-1-3 scheme has the highest and the 1-2-2 scheme has the lowest deflection for all values of power-law index. It is to be marked that the 4-1-3 scheme is constituted of the thinnest, whereas, the 1-2-2 scheme is constituted of the thickest core and thereby influencing the

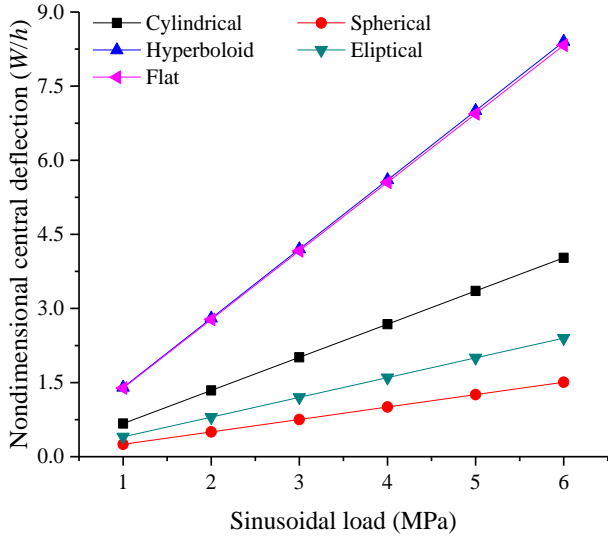


Fig. 10 Influence of geometry on nondimensional central deflection

stiffness and consequently the central deflection values of the panels.

### 3.3.5 Effect of geometry

To study the influence of geometry on the flexural responses the central deflection values of simply supported cylindrical, spherical, elliptical, hyperboloid and flat FG sandwich shell panels ( $h_c/h_f=3$  and  $k=2$ ) are computed for varying sinusoidal load and plotted in Fig. 10. Additionally, the nondimensional normal and transverse stresses are obtained for the considered geometries corresponding to  $q_0=1$  MPa and illustrated in Fig. 11. It is observed that the central deflection increases with increasing load irrespective of the geometries. However, it is worthy to note that the deflection increases as the curvature of the panels increases and the spherical shell panels exhibit least deflection of all the considered geometries. It is interesting to note that the deflection for hyperboloid and flat shell panels are in close proximity of each other. This is attributed to fact that the

presence of positive and negative curvature (the centre of curvatures lie on the opposite sides of the panel) in the hyperboloid panel that make it resemble the flat panels. A similar trend is observed from the plot of nondimensional normal and transverse stresses plotted in Fig. 11(a) and (b), respectively.

### 3.3.6 Effect of curvature ratio

The influence of five different curvature ratios ( $R/a = 1, 2, 5, 10$  and  $25$ ) on the deflection behaviour of simply supported shell structures (cylindrical, spherical, elliptical and hyperboloid) are investigated and presented in Fig. 12(a) and (b). The variation of curvature ratio ( $R/a$ ) are obtained by changing the values of ' $R$ ' keeping ' $a$ ' constant. The deflection values of the three shell panels (cylindrical, spherical and elliptical) are following an increasing line. However, the curvature ratio has insignificant effect for the hyperboloid shell structure. Additionally, the deflection responses are significant for the small values of curvature ratios in comparison to the higher  $R/a$ , irrespective of geometrical configurations. Moreover, the deflection values are higher for the lower core-to-face thickness ratios for each type of geometries and results follow the expected line.

### 3.3.7 Effect of support conditions

Finally, the influence of support conditions on the flexural behaviour of FG sandwich curved shell panels ( $h_c/h_f=3$  and  $k=2$ ) is investigated. As expected, the number of constraints at the supports alters the stiffness of the panels. The spherical and elliptical panels (doubly curved) have lesser deflection compared to cylindrical and hyperboloid panels due to higher stiffness caused by curvature and the same can be observed from Fig. 13(a) and (b). The deflection increases with increasing sinusoidal load. Further, the [CCCC] condition has the least, whereas, the [SSSS] condition has the highest central deflection irrespective of the geometries of the panel considered. The [HHHH] condition is stiffer compared to [SCSC] condition and consequently the deflection is smaller in the former condition.

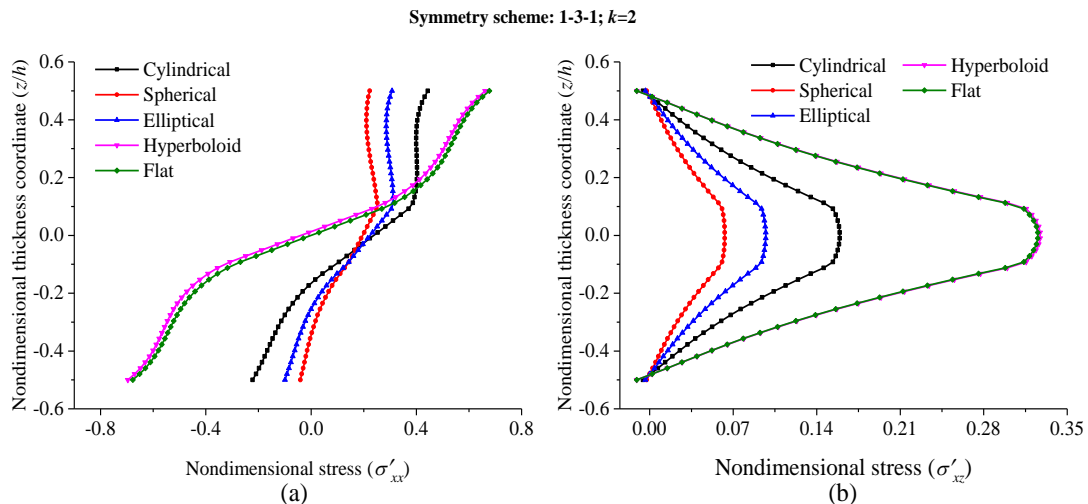


Fig. 11 Variation of nondimensional stress with thickness: (a) Normal stress, (b) Shear stress

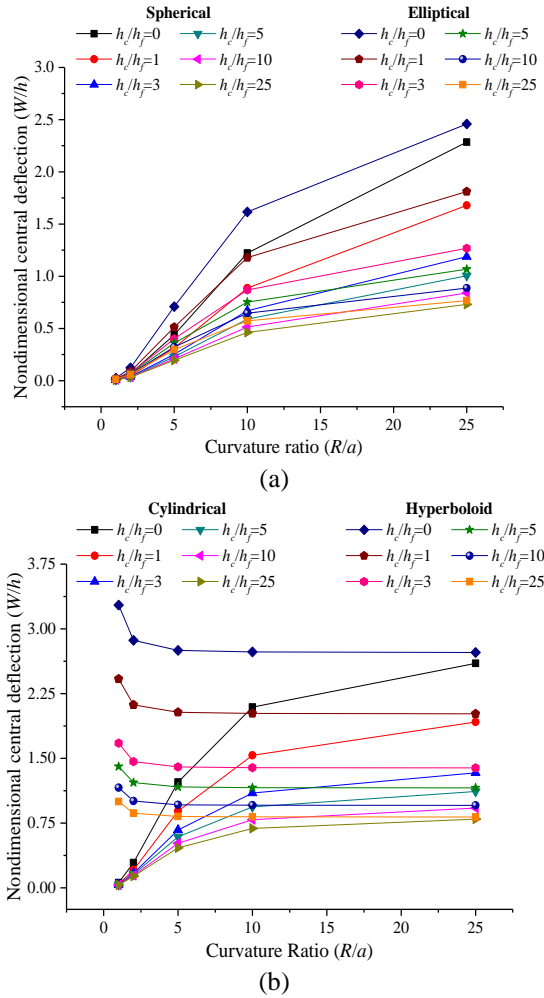


Fig. 12 Influence of curvature on nondimensional central deflection: (a) Spherical and elliptical panels, (b) Cylindrical and hyperboloid panels

#### 4. Conclusions

In this paper, the flexural behaviour of FG sandwich curved shell panels have been investigated using the HOSDT based mid-plane kinematic model constituting of nine degrees of freedom and implemented via own FE code developed in MATLAB environment. The core is considered to be made of ceramic whereas the faces are functionally graded. The convergence and validation study demonstrated that the present formulation yields valid and reliable estimate of the flexural responses of FG sandwich shell panels. From the extensive parametric study performed using the present model it is observed that the central deflection values increase with increasing power-law index values as well as the thickness ratio whereas decreases with increasing number of constraints at the supports. However, as the core-face thickness ratio increases, the stiffness of the panels increases due to the core becoming thicker and consequently the deflection of the panels decreases. The spherical panels are the stiffest due to the presence of equal curvatures along the longitudinal as well as transverse directions. The sandwich symmetry scheme 4-1-3 contributes to maximum deflection

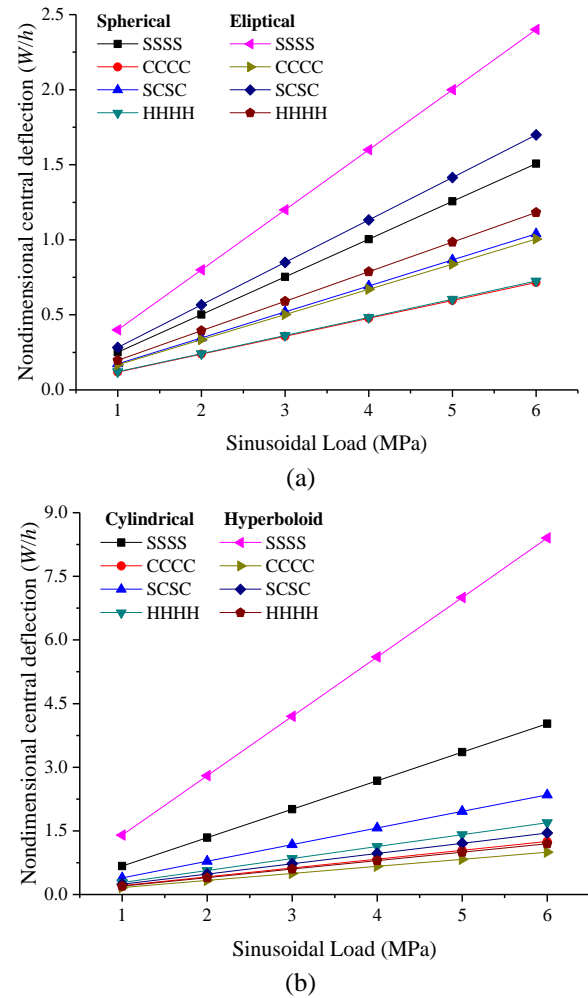


Fig. 13 Influence of support conditions on nondimensional central deflection: (a) Spherical and elliptical panels, (b) Cylindrical and hyperboloid panels

amongst all of the schemes considered. The central deflection for all the geometries increases with increasing curvature ratio whereas a reverse trend is noticed in the case of the hyperboloid panels.

#### References

- Abdelaziz, H.H., Atmane, H.A., Mechab, I., Boumia, L., Tounsi, A. and El Abbas, A.B. (2011), "Static analysis of functionally graded sandwich plates using an efficient and simple refined theory", *Chin. J. Aeronaut.*, **24**, 434-448.
- Abualnour, M., Houari, M.S.A., Tounsi, A. and Mahmoud, S.R. (2018), "A novel quasi-3D trigonometric plate theory for free vibration analysis of advanced composite plates", *Compos. Struct.*, **184**, 688-697.
- Yahia, S.A., Atmane, H.A., Houari, M.S.A. and Tounsi, A. (2015), "Wave propagation in functionally graded plates with porosities using various higher-order shear deformation plate theories", *Struct. Eng. Mech.*, **53**(6), 1143-1165.
- Alipour, M.M. and Shariyat, M. (2012), "An elasticity-equilibrium-based zigzag theory for axisymmetric bending and stress analysis of the functionally graded circular sandwich plates, using a Maclaurin-type series solution", *Eur. J. Mech.*

- A/Solid.*, **34**, 78-101.
- Anderson, T.A. (2003), "A 3-D elasticity solution for a sandwich composite with functionally graded core subjected to transverse loading by a rigid sphere", *Compos. Struct.*, **60**, 265-274.
- Attia, A., Bousahla, A.A., Tounsi, A., Mahmoud, S.R. and Alwabri, A.S. (2018), "A refined four variable plate theory for thermoelastic analysis of FGM plates resting on variable elastic foundations", *Struct. Eng. Mech.*, **65**(4), 453-464.
- Ayache, B., Bennai, R., Fahsi, B., Fourn, H., Atmane, H.A. and Tounsi, A. (2018), "Analysis of wave propagation and free vibration of functionally graded porous material beam with a novel four variable refined theory", *Earthq. Struct.*, **15**(4), 369-382.
- Baseri, V., Jafari, G.S. and Kolahchi, R. (2016), "Analytical solution for buckling of embedded laminated plates based on higher order shear deformation plate theory", *Steel Compos. Struct.*, **21**, 883-919.
- Belabed, Z., Bousahla, A.A., Houari, M.S.A., Tounsi, A. and Mahmoud, S.R. (2018), "A new 3-unknown hyperbolic shear deformation theory for vibration of functionally graded sandwich plate", *Earthq. Struct.*, **14**(2), 103-115.
- Belabed, Z., Houari, M.S.A., Tounsi, A., Mahmoud, S.R. and Bég, O.A. (2014), "An efficient and simple higher order shear and normal deformation theory for functionally graded material (FGM) plates", *Compos. Part B*, **60**, 274-283.
- Bellifa, H., Benrahou, K.H., Hadji, L., Houari, M.S.A. and Tounsi, A. (2016), "Bending and free vibration analysis of functionally graded plates using a simple shear deformation theory and the concept the neutral surface position", *J. Brazil. Soc. Mech. Sci. Eng.*, **38**(1), 265-275.
- Bellifa, H., Bakora, A., Tounsi, A., Bousahla, A.A. and Mahmoud, S.R. (2017), "An efficient and simple four variable refined plate theory for buckling analysis of functionally graded plates", *Steel Compos. Struct.*, **25**(3), 257-270.
- Benadouda, M., Atmane, H.A., Tounsi, A., Bernard, F. and Saeed, M.S. (2018), "An efficient shear deformation theory for wave propagation in functionally graded material beams with porosities", *Earthq. Struct.*, **13**(3), 255-265.
- Bennoun, M., Houari, M.S.A. and Tounsi, A. (2016), "A novel five-variable refined plate theory for vibration analysis of functionally graded sandwich plates", *Mech. Adv. Mater. Struct.*, **23**(4), 423-431.
- Bouderba, B., Houari, M.S.A., Tounsi, A. and Mahmoud, S.R. (2016), "Thermal stability of functionally graded sandwich plates using a simple shear deformation theory", *Struct. Eng. Mech.*, **58**(3), 397-422.
- Boukhari, A., Atmane, H.A., Tounsi, A., Adda, B. and Mahmoud, S.R. (2016), "An efficient shear deformation theory for wave propagation of functionally graded material plates", *Struct. Eng. Mech.*, **57**(5), 837-859.
- Bousahla, A.A., Benyoucef, S., Tounsi, A. and Mahmoud, S.R. (2016), "On thermal stability of plates with functionally graded coefficient of thermal expansion", *Struct. Eng. Mech.*, **60**(2), 313-335.
- Bousahla, A.A., Houari, M.S.A., Tounsi, A. and Adda Bedia, E.A. (2014), "A novel higher order shear and normal deformation theory based on neutral surface position for bending analysis of advanced composite plates", *Int. J. Comput. Meth.*, **11**(6), 1350082.
- Chaht, F.L., Kaci, A., Houari, M.S.A., Tounsi, A., Bég, O.A. and Mahmoud, S.R. (2015), "Bending and buckling analyses of functionally graded material (FGM) size-dependent nanoscale beams including the thickness stretching effect", *Steel Compos. Struct.*, **18**(2), 425-442.
- Cook, R.D., Malkus, D.S. and Plesha, M.E. (2000), *Concepts and Applications of Finite Element Analysis*, 3rd Edition, Singapore: John Wiley and Sons.
- Das, M., Barut, A., Madenci, E. and Ambur, D.R. (2006), "A triangular plate element for thermo-elastic analysis of sandwich panels with a functionally graded core", *Int. J. Numer. Meth. Eng.*, **68**, 940-966.
- Draiche, K., Tounsi, A. and Mahmoud, S.R. (2016), "A refined theory with stretching effect for the flexure analysis of laminated composite plates", *Geomech. Eng.*, **11**(5), 671-690.
- El-Haina, F., Bakora, A., Bousahla, A.A., Tounsi, A. and Mahmoud, S.R. (2017), "A simple analytical approach for thermal buckling of thick functionally graded sandwich plates", *Struct. Eng. Mech.*, **63**(5), 585-595.
- Fourn, H., Atmane, H.A., Bourada, M., Bousahla, A.A., Tounsi, A. and Mahmoud, S.R. (2018), "A novel four variable refined plate theory for wave propagation in functionally graded material plates", *Steel Compos. Struct.*, **27**(1), 109-122.
- Ghannadpour, S.A.M., Ovesy, H.R. and Nassirnia, M. (2012), "Buckling analysis of functionally graded plates under thermal loadings using the finite strip method", *Comput. Struct.*, **108-109**, 93-99.
- Hamidi, A., Houari, M.S.A., Mahmoud, S.R. and Tounsi, A. (2015), "A sinusoidal plate theory with 5-unknowns and stretching effect for thermomechanical bending of functionally graded sandwich plates", *Steel Compos. Struct.*, **18**(1), 235-253.
- Houari, M.S.A., Tounsi, A. and Bég, O.A. (2013), "Thermoelastic bending analysis of functionally graded sandwich plates using a new higher order shear and normal deformation theory", *Int. J. Mech. Sci.*, **76**, 102-111.
- Jha, D.K., Kant, T. and Singh, R.K. (2012), "A critical review of recent research on functionally graded plates", *Compos. Struct.*, **96**, 833-849.
- Kant, T. and Swaminathan, K. (2002), "Analytical solutions for the static analysis of laminated composite and sandwich plates based on a higher order refined theory", *Compos. Struct.*, **56**, 329-344.
- Karami, B., Janghorban, M. and Tounsi, A. (2018), "Variational approach for wave dispersion in anisotropic doubly-curved nanoshells based on a new nonlocal strain gradient higher order shell theory", *Thin Wall. Struct.*, **129**, 251-264.
- Kashtalyan, M. and Menshykova, M. (2007), "Three-dimensional elasticity solution for sandwich panels with a functionally graded core", *Compos. Struct.*, **87**, 36-43.
- Kolahchi, R. (2017), "A comparative study on the bending, vibration and buckling of viscoelastic sandwich nano-plates based on different nonlocal theories using DC, HDQ and DQ methods", *Aerosp. Sci. Technol.*, **66**, 235-248.
- Arani, A.J. and Kolahchi, R. (2016), "Buckling analysis of embedded concrete columns armed with carbon nanotubes", *Comput. Concrete*, **17**(5), 567-578.
- Kolahchi, R., Zarei, M.S., Hajmohammad, M.H. and Oskouei, A.N. (2017b), "Visco-nonlocal-refined Zigzag theories for dynamic buckling of laminated nanoplates using differential cubature-Bolotin methods", *Thin Wall. Struct.*, **113**, 162-169.
- Kolahchi, R., Hosseini, H. and Esmailpour, M. (2016), "Differential cubature and quadrature-Bolotin methods for dynamic stability of embedded piezoelectric nanoplates based on visco-nonlocal-piezoelectricity theories", *Compos. Struct.*, **157**, 174-186.
- Kolahchi, R., Zarei, M.S., Hajmohammad, M.H. and Nouri, A. (2017a), "Wave propagation of embedded viscoelastic FG-CNT-reinforced sandwich plates integrated with sensor and actuator based on refined zigzag theory", *Int. J. Mech. Sci.*, **130**, 534-545.
- Kolahchi, R. and Heydari, M.M. (2015), "Size-dependent bending analysis of FGM nano-sinusoidal plates resting on orthotropic elastic medium", *Struct. Eng. Mech.*, **55**, 1001-1014.
- Lok, T.S. and Cheng, Q.H. (2001), "Bending and forced vibration response of a clamped orthotropic thick plate and sandwich

- panel", *J. Sound Vib.*, **245**, 63-78.
- Mahi, A., Bedia, E.A.A. and Tounsi, A. (2015), "A new hyperbolic shear deformation theory for bending and free vibration analysis of isotropic, functionally graded, sandwich and laminated composite plates", *Appl. Math. Model.*, **39**, 2489-2508.
- Mahmoudi, A., Benyoucef, S., Tounsi, A., Benachour, A. and Bedia, E.A.A. (2018), "On the effect of the micromechanical models on the free vibration of rectangular FGM plate resting on elastic foundation", *Earthq. Struct.*, **14**(2), 117-128.
- Meziane, M.A.A., Abdelaziz, H.H. and Tounsi, A. (2014), "An efficient and simple refined theory for buckling and free vibration of exponentially graded sandwich plates under various boundary conditions", *J. Sandw. Struct. Mater.*, **16**, 293-318.
- Menasria, A., Bouhadra, A., Tounsi, A., Bousahla, A.A. and Mahmoud, S.R. (2017), "A new and simple HSDT for thermal stability analysis of FG sandwich plates", *Steel Compos. Struct.*, **25**(2), 157-175.
- Natarajan, S., Haboussi, M. and Manickam, G. (2014), "Application of higher-order structural theory to bending and free vibration analysis of sandwich plates with CNT reinforced composite facesheets", *Compos. Struct.*, **113**, 197-207.
- Natarajan, S. and Ganapathi, M. (2012), "Bending and vibration of functionally graded material sandwich plates using an accurate theory", *Finite Elem. Anal. Des.*, **52**, 32-42.
- Neves, A.M.A., Ferreira, A.J.M., Carrera, E., Cinefra, M., Jorge, R.M.N. and Soares, C.M.M. (2012), "Static analysis of functionally graded sandwich plates according to a hyperbolic theory considering Zig-Zag and warping effects", *Adv. Eng. Softw.*, **52**, 30-43.
- Neves, A.M.A., Ferreira, A.J.M., Carrera, E., Cinefra, M., Roque, C.M.C. and Jorge, R.M.N. (2012), "Static, free vibration and buckling analysis of isotropic and sandwich functionally graded plates using a quasi-3D higher-order shear deformation theory and a meshless technique", *Compos. Part B*, **44**, 657-674.
- Nguyen-Xuan, H., Thai, C.H. and Nguyen-Thoi, T. (2013), "Isogeometric finite element analysis of composite sandwich plates using a higher order shear deformation theory", *Compos. Part B*, **55**, 558-574.
- Ovesy, H.R., Ghannadpour, S.A.M. and Nassirnia, M. (2015), "Post-buckling analysis of rectangular plates comprising Functionally Graded Strips in thermal environments", *Comput. Struct.*, **147**, 209-215.
- Sekkal, M., Fahsi, B., Tounsi, A. and Mahmoud, S.R. (2017), "A novel and simple higher order shear deformation theory for stability and vibration of functionally graded sandwich plate", *Steel Compos. Struct.*, **25**(4), 389-401.
- Sherafat, M.H., Ovesy, H.R. and Ghannadpour, S.A.M. (2013), "Buckling analysis of functionally graded plates under mechanical loading using higher order functionally graded strip", *Int. J. Struct. Stab. Dyn.*, **13**, 1350033-1-13.
- Sobhy, M. and Zenkour, A.M. (2015), "Thermodynamical bending of FGM sandwich plates resting on Pasternak's elastic foundations thermodynamical bending of FGM sandwich plates resting on Pasternak's elastic foundations introduction sandwich structures have high structural efficiency because", *Adv. Appl. Math. Mech.*, **7**, 116-134.
- Thai, H.T., Nguyen, T.K., Vo, T.P. and Lee, J. (2014), "Analysis of functionally graded sandwich plates using a new first-order shear deformation theory", *Eur. J. Mech. A/Solid.*, **45**, 211-225.
- Thai, H.T. and Kim, S.E. (2015), "A review of theories for the modeling and analysis of functionally graded plates and shells", *Compos. Struct.*, **128**, 70-86.
- Vinson, J.R. (2001), "Sandwich structure", *Appl. Mech. Rev.*, **54**, 201-214.
- Wang, Z.X. and Shen, H.S. (2011), "Nonlinear analysis of sandwich plates with FGM face sheets resting on elastic foundations", *Compos. Struct.*, **93**, 2521-2532.
- Yang, J., Kitipornchai, S. and Liew, K.M. (2008), "Nonlinear local bending of FGM sandwich plates", *J. Mech. Mater. Struct.*, **3**, 1977-1922.
- Younsi, A., Tounsi, A., Zaoui, F.Z., Bousahla, A.A. and Mahmoud, S.R. (2018), "Novel quasi-3D and 2D shear deformation theories for bending and free vibration analysis of FGM plates", *Geomech. Eng.*, **14**(6), 519-532.
- Zenkour, A.M. and Alghamdi, N.A. (2008), "Thermoelastic bending analysis of functionally graded sandwich plates", *J. Mater. Sci.*, **43**, 2574-89.
- Zenkour, A.M. (2005a), "A comprehensive analysis of functionally graded sandwich plates : Part 1-Deflection and stresses", *Int. J. Solid. Struct.*, **42**, 5224-42.
- Zenkour, A.M. (2005b), "A comprehensive analysis of functionally graded sandwich plates : Part 2-Buckling and free vibration", *Int. J. Solid. Struct.*, **42**, 5243-5258.
- Zenkour, A.M. (2013), "Bending analysis of functionally graded sandwich plates using a simple four-unknown shear and normal deformations theory", *J. Sandw. Struct. Mater.*, **15**, 629-656.
- Zenkour, A.M. and Alghamdi, N.A. (2010), "Bending analysis of functionally graded sandwich plates under the effect of mechanical and thermal loads", *Mech. Adv. Mater. Struct.*, **17**, 419-432.
- Zine, A., Tounsi, A., Draiche, K., Sekkal, M. and Mahmoud, S.R. (2018), "A novel higher-order shear deformation theory for bending and free vibration analysis of isotropic and multilayered plates and shells", *Steel Compos. Struct.*, **26**(2), 125-137.

CC